Oxidation of palladium powder by the adduct Ph2P(S)NHP(S)Ph2·I2. Crystal structure of PdL2

G. Luca Abbati,[a] M. Carla Aragoni,[b] Massimiliano Arca,[b] Francesco A. Devillanova,[b] Antonio C. Fabretti,[a] Alessandra Garau,[b] Francesco Isaia*[b] Vito Lippolis[b] and Gaetano Verani[b]

[a] *Dipartimento di Chimica, Università di Modena e Reggio Emilia, Via G. Campi 183, I-41100, Modena, Italy*
[b] *Dipartimento di Chimica Inorganica ed Analitica, Università di Cagliari, SS 554 bivio per Sestu, I-09042, Cagliari, Italy. E-mail: isaia@unica.it*

The reaction of palladium powder with the diiodine adduct of $Ph_2P(S)NHP(S)Ph_2$ (**HL**) in Et_2O gave the complex $Pd(HL)I_2$ **1**. Subsequent crystallisation from CH_3CN separates the complex PdL_2. Its crystal structure comprises discrete, monomeric molecules where a Pd^{II} is in a square planar geometry coordinated to four sulfur atoms of two bidentate anionic ligands. The electrochemistry of $HL·I_2$ and PdL_2 has been studied by cyclic voltammetry. FT-IR and ^{31}P NMR spectroscopies are in accordance with the nature of the ligand in the two complexes. Hybrid-DFT calculations have been performed on a model complex $Pd[H_2P(S)NP(S)H_2]_2$ to gain insight on the electronic nature of PdL_2.

Introduction

In recent years the oxidation reaction of metal powders by diiodine adducts with P, S, Se donor molecules has proved valuable in the synthesis of coordination compounds having unusual geometries, stoichiometries, and oxidation numbers at the metal centres.[1] For example, with the powerful reagent $R_3P·I_2$ (R = Me, Et, Pr^n or Bu^n), Godfrey and co-workers have been able to oxidise not only Co and Ni to the +3 oxidation state,[1d] but also gold powder to Au^{III}.[1a] Metal activation reactions using the adducts of polyfunctional thione donors with I_2 have also been studied: in the case of the reaction of the bis-diiodine adduct of N,N'-dimethylperhydrodiazepine-2,3-dithione (D) with gold powder, an interesting gold(III) complex $[AuDI_2]I_3$ was easily prepared,[1b] whereas the bis-diiodine adduct of 1,1'-bis(3-methyl-4-imidazolidine-2-thione)methane (D') reacts with tin powder to produce the tin(IV) complex $SnI_2(D')_2(I_3)_2·\frac{2}{3}I_2$.[1c]

In this context diiodine adducts of phosphine sulfide compounds represent interesting systems for activating metals, since they contain both 15 and 16 Group donor elements. Amongst phosphine sulfide derivatives the bis(dialkylthiophosphoryl)-amines $R_2P(S)NHP(S)R'_2$ (R, R' = Me, Pr^i or Ph) have recently received great attention as demonstrated by the large number of papers reporting on the coordination chemistry of these bidentate ligands.[2] The reaction of $Ph_2P(S)NHP(S)Ph_2$ (**HL**) with metal ions usually leads to deprotonation of the NH group and consequent formation of the anionic ligand $[Ph_2P(S)NP(S)Ph_2]^-$ (**L**). This tends to coordinate either as a bidentate chelate to form square planar, tetrahedral or octahedral complexes of general formula ML_n (n = 1, 2 or 3),[3] or as found in a variety of complexes of rare-earth metals through two sulfur atoms and a nitrogen atom.[4] In some cases, even more complicated stoichiometries have been observed with formation of bridges or supramolecular polymeric structures.[5]

With the aim of testing the potential oxidation ability of $HL·I_2$ towards metal powders in a low polar solvent such as diethyl ether, and in order to study the coordination compounds that can be obtained, we have recently examined the synthesis and structural characterisation of an unusual

dinuclear complex $[LSb(\mu-S)(\mu-I)_2SbL]$ starting from Sb^0.[5a] In this complex the antimony(III) ions show a slightly distorted square pyramidal geometry achieved by one bidentate **L** molecule and three bridged anions (two I^- and one S^{2-}). The oxidising ability of the $HL·I_2$ reagent led the antimony to the +3 oxidation state in a single oxidation step. Similarly, the reaction of $HL·I_2$ with cobalt powder[3a] produced the complex CoL_2, however the reagent did not show the ability further to oxidise the metal centre to the +3 oxidation state.

Considering these results and in view of the new perspectives shown by this synthetic route in the recovery of precious metals either from exhausted catalysts or in the metal refining industry,[1b] we have extended the use of the $HL·I_2$ adduct as oxidising agent towards Group 10 metals and now report on the results obtained with palladium.

Experimental

Materials and instrumentation

Reagents were used as purchased from Aldrich. Diethyl ether was distilled over $LiAlH_4$ shortly before use. All reactions were carried out under a dry nitrogen atmosphere.

$^{31}P-\{^1H\}$ NMR spectra were recorded on a Varian Unity Inova 400 MHz spectrometer operating at 161.9 MHz. The ^{31}P chemical shifts were calibrated indirectly through the 85% H_3PO_4 peak (δ 0.0). IR spectra were measured as KBr (4000–400 cm^{-1}) and polyethylene pellets (400–50 cm^{-1}) on a Bruker IFS 55 FT-IR spectrometer. Cyclic voltammetry experiments were recorded at room temperature, in anhydrous CH_2Cl_2, at a scan rate of 100 mV s^{-1}, using a conventional three-electrode cell, consisting of a combined working and counter platinum electrode and a standard Ag–AgCl (in 3.5 mol dm^{-3} KCl; 0.2050 V) reference electrode. The solution was about 1×10^{-3} mol dm^{-3} in the complex or $HL·I_2$, with $Bu_4^nNBF_4$ (0.1 mol dm^{-3}) as supporting electrolyte. A stream of argon was passed through the solution prior to the scan. Data were recorded on a computer-controlled EG&G (Princeton Applied Research) potentiostat-galvanostat Model 273 EG&G, using Model 270 electrochemical analysis software. EI mass spectra were

run on a Fisons QMD 1000 instrument operating in the EI$^+$ mode.

Synthesis

Compound Ph$_2$P(S)NHP(S)Ph$_2$ (**HL**) was prepared according to ref. 6. Adducts Ph$_2$P(S)NHP(S)Ph$_2$·IX (X = I, Br or Cl) were prepared *in situ* in Et$_2$O or other solvents just before use from a 1 : 1 Ph$_2$P(S)NHP(S)Ph$_2$: IX molar ratio.

Pd[Ph$_2$P(S)NHP(S)Ph$_2$]I$_2$ 1. A mixture of **HL** (100.0 mg, 0.222 mmol) and I$_2$ (56.5 mg, 0.223 mmol) in diethyl ether (200 ml) was stirred at room temperature under N$_2$ until complete dissolution of the reagents. Finely milled palladium metal powder (23.6 mg, 0.222 mmol) was then added while stirring. This was continued at room temperature under N$_2$ for *ca*. 21 days. The resulting air-stable brownish solid **1** was isolated by suction filtration, washed with diethyl ether, and dried *in vacuo*. Yield 0.172 g, 0.211 mmol, 95%. Found: C, 35.1; H, 2.5; N, 1.7; S, 8.1%. Calc. for C$_{24}$H$_{21}$I$_2$NP$_2$PdS$_2$: C, 35.60; H, 2.61; N, 1.73; S, 7.92%. IR (KBr, cm^{-1}): 2560w, 1726w, 1584w, 1571w, 1481w, 1437vs, 1335w, 1294vs, 1261vs, 1187w, 1103vs, 1025s, 915vs, 800vs, 745s, 739s, 716s, 705ms, 685s, 616w, 598ms, 587vs and 489s. EI MS: *m/z* 809; calc. for ^{106}Pd[Ph$_2$P(S)NHP(S)Ph$_2$]I$_2$: *m/z* 809.31. ^{31}P NMR (CD$_3$CN): δ 56.3.

Pd[Ph$_2$P(S)NHP(S)Ph$_2$]Br$_2$ 2. A similar procedure produced complex **2** after *ca*. 7 days, when an equimolar amount of IBr was used instead of I$_2$. Yield 0.055 g, 0.077 mmol, 35%. Found: C, 35.1; H, 2.5; N, 1.7; S, 8.1%. Calc. for C$_{24}$H$_{21}$Br$_2$NP$_2$PdS$_2$: C, 40.28; H, 2.96; N, 1.96; S, 8.96%. IR (KBr, cm^{-1}): 1583w, 1481w, 1437vs, 1311s, 1248s, 1184w, 1162w, 1114vs, 1106vs, 1027w, 995w, 874s, 814ms, 748vs, 725s, 712s, 685s, 616w, 584vs, 513s, 485ms and 454ms. ^{31}P NMR (CD$_3$CN): δ 55.7.

Pd[Ph$_2$P(S)NP(S)Ph$_2$]$_2$ 3. Solid complex **1** (50 mg, 0.111 mmol) was dissolved in hot CH$_3$CN (100 ml); the filtered solution was allowed to concentrate at room temperature. Well shaped brown-red crystals of **3** were obtained in a few days. Yield 0.045 g, 0.044 mmol, 40%. Found: C, 57.6; H, 4.1; N, 2.8; S, 13.0%. Calc for C$_{48}$H$_{40}$N$_2$P$_4$PdS$_4$: C, 57.46; H, 4.02; N, 2.79; S, 12.78%. IR (KBr, cm^{-1}): 3050w, 1161s, 1110s, 1025m, 998m, 821ms, 745ms,717ms, 701vs, 617w, 571vs, 565vs, 526w, 512ms, 407m and 396m. ^{31}P NMR (CDCl$_3$): δ 38.7.

X-Ray crystallography

Crystal data for complex 3. C$_{48}$H$_{40}$N$_2$P$_4$PdS$_4$, M = 1003.41, triclinic, space group[7] $P\bar{1}$ (no. 2), a = 8.8384(10), b = 11.516(2), c = 13.328(2) Å, α = 112.140(10), β = 100.220(10), γ = 105.204(11)°, U = 1153.1(3) Å^3, T = 293(2) K, Z = 1, μ(Mo-Kα) = 0.758 mm^{-1}, 4550 reflections collected, 4385 unique (R_{int} = 0.0205) which were used in all calculations.

Data were collected at room temperature on an Enraf Nonius-CAD4 automatic diffractometer, using graphite monochromated Mo-Kα radiation (λ = 0.71073 Å). All data were corrected for Lorentz-polarisation effects and an empirical absorption correction, based on ψ scans, was applied.[8a] The structure was solved by direct methods (SIR 92)[8b] and refined on F_o^2 employing the full-matrix least-squares calculation technique with the SHELXL 93 software package.[8c] Anisotropic thermal parameters were refined for all non-hydrogen atoms, while the hydrogen atoms, localised in the last steps of the refinement from the ΔF map, were refined isotropically. The structure refinement converged to final agreement factors (on all data) $R1$ = 0.0389 and $wR2$ = 0.0821. Selected interatomic distances and angles are listed in Table 1. All calculations were carried out on an Alpha 3000/800S computer.

CCDC reference number 153387.

See http://www.rsc.org/suppdata/dt/b0/b009286j/ for crystallographic data in CIF or other electronic format.

Computations

Quantum-chemical calculations were carried out using the commercially available suite of programs GAUSSIAN 94.[9a] Density Functional Theory (DFT)[9b] calculations were performed using the hybrid B3LYP functional (which uses a mixture[9c] of Hartree–Fock and DFT exchange along with DFT correlation: the Lee–Yang–Parr correlation functional[9e] together with Becke's gradient correction[9d]). The pVDZ basis set of Schafer *et al.*[9f] was used for C, H, N, P and S, while the Hay–Wadt basis set with effective core potentials (ECP)[9g,h] was used for the heavier Pd atom. Integration was performed numerically using a total of 7500 points for each atom (Finegrid option). Starting from geometrical parameters determined for complex **3**, and avoiding introducing any geometrical constraints, a geometry optimisation was performed and the results of the calculations were examined with the MOLDEN 3.6 program.[9i] The quantum mechanically optimised structure was verified by normal-mode harmonic frequency analysis. Harmonic frequencies were obtained using the second derivatives of the DFT energy, computed by numerical differentiation of the DFT energy gradients. The qualitative EHT[9j] analyses were obtained with the CACAO (Computer Aided Composition of Atomic Orbitals) program package[9k] on the Hybrid-DFT optimised geometry. The interaction diagram was generated using the fragment molecular orbital (FMO) approach.[9l] Parameters used in EHT calculations were taken from the standard database of CACAO.

Results and discussion

Synthesis and ^{31}P NMR studies

The reaction between **HL**, I$_2$ and palladium metal powder (1 : 1 : 1 molar ratio) in anhydrous diethyl ether gives a brownish solid product having elemental analysis and mass spectra in agreement with a stoichiometry PdI$_2$·HL **1**. In this reaction the zero-valent palladium is oxidised to Pd^{II} according to eqn. (1)

$$Ph_2P(S)NHP(S)Ph_2 + I_2 + Pd \xrightarrow{\text{Et}_2\text{O}}$$
$$Pd[Ph_2P(S)NHP(S)Ph_2]I_2 \quad (1)$$
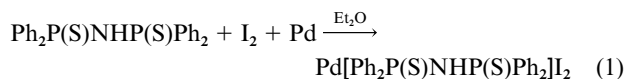
^{31}P NMR spectra of the mixture, recorded several times during a three-week period, show that during the reaction the reagent **HL**·I$_2$ (δ 57.4, Et$_2$O), whose amount in solution decreases with time, is the only phosphorus-containing species present, due to the very low solubility of complex **1** in Et$_2$O. The ^{31}P NMR spectrum of **1** in CD$_3$CN solvent, in which this complex is partly soluble, consists of a single broad peak at δ 56.3. This chemical shift value indicates the presence of the ligand in its protonated form in the complex, as deprotonation of the ligand results in a shift of the ^{31}P NMR signal to lower frequency by *ca*. 20–30 ppm.[2f] No low-temperature experiments could be made to look into any dynamic process within the ligand on account of its low solubility. The ^{31}P NMR chemical shift found for **1** is comparable to that for PdBr$_2$·HL (**2**) (δ 55.7, CD$_3$CN), which to our knowledge is the only other known palladium complex containing the neutral ligand **HL**. Although McQuillan and Oxton were able to synthesize **2** by treating K$_2$PdBr$_4$ with **HL** in acidified acetone,[10] they failed to obtain other complexes of the same type, since when other starting palladium salts were used the dissociation of the imido proton was easy and led to immediate precipitation of the PdL$_2$ **3** species. We were able to prepare complex **2** by treating the adduct **HL**·IBr with palladium powder in Et$_2$O, but failed to prepare any complex when we used **HL**·ICl because of the intrinsic instability of this adduct. In fact, ^{31}P NMR spectra of **HL**·IX (X = I, Br or Cl) in Et$_2$O recorded 48 h after being prepared (25 °C) show that the **HL**·I$_2$ species is completely stable, whereas only 85 and 44% of the initial amounts of **HL**·IBr and
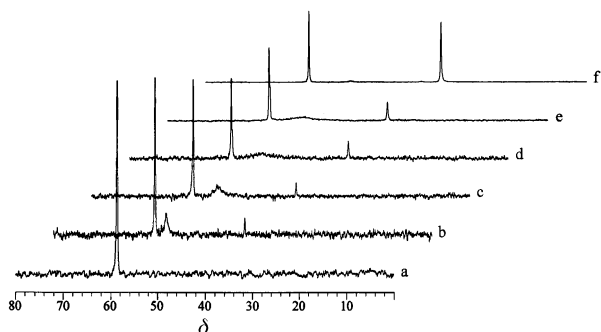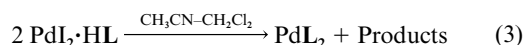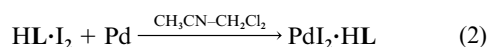
Fig. 1 ^{31}P NMR spectra at 25 °C of the reaction mixture of HL·I$_2$ (1.11 mM) in CH$_3$CN–CH$_2$Cl$_2$ (1 : 1 v:v) with the palladium powder in a 2 : 1 molar ratio after 0, 2, 4, 6, 10, and 14 days, denoted as a, b, c, d, e, and f, respectively.

HL·ICl, respectively, are still present in the solution, since these adducts are to some extent unstable compared to the imido proton dissociation.

Reaction (1) was also carried out in Et$_2$O using an excess of HL·I$_2$ in order to achieve a higher oxidation state of the palladium or synthesize complexes with a higher content of ligand, but **1** remained the only isolated species. Probably, the very low solubility of **1** prevents its further reaction with HL·I$_2$.

Thus, the reaction was carried out using a Pd : HL·I$_2$ 1 : 2 reaction molar ratio in the mixture CH$_3$CN–CH$_2$Cl$_2$ (1 : 1 v:v), where **1** is soluble. It was monitored by ^{31}P NMR (Fig. 1). Initially, HL·I$_2$ (δ 58.6) reacts with palladium powder to form a new species, which shows a signal at δ 56.5. Assignment of this signal to complex **1** is straightforward and supported by comparison with the spectra of the neat compound recorded in CH$_3$CN, δ 56.3. In the course of the reaction the ^{31}P NMR signal related to **1** broadens and shifts to highfield until it reaches the noise level; at the same time, formation of a new signal at δ 36.5, which can be related to a deprotonated ligand-containing species, is observed. After two weeks the solution undergoes no further changes. Only two signals are detectable with a 1 : 1 relative intensity corresponding to nearly half the initial amount of HL·I$_2$, and to the above mentioned new species. After three weeks, partial removal of the solvent yielded an orange powder, whose crystallisation from hot CH$_3$CN yielded orange crystals having the stoichiometry PdL$_2$ **3**. The ^{31}P NMR spectrum of **3** (CDCl$_3$) features only one narrow band (showing the equivalence of the four phosphorus atoms) at δ 38.7. Low-temperature measurements were carried out as far as −40 °C, the lowest temperature for which ^{31}P NMR data were recordable, with no significant change in the spectra suggesting the presence of different conformers.

Based on ^{31}P NMR data it can be hypothesised that the reaction carried out in the mixture CH$_3$CN–CH$_2$Cl$_2$ occurs in two steps, the first of which leads to the formation of complex **1** which subsequently evolves to the more stable species **3**, eqns. (2) and (3). Complex **3**, which is soluble in CH$_2$Cl$_2$, was

$$\text{HL·I}_2 + \text{Pd} \xrightarrow{\text{CH}_3\text{CN–CH}_2\text{Cl}_2} \text{PdI}_2\text{·HL} \qquad (2)$$

$$2\ \text{PdI}_2\text{·HL} \xrightarrow{\text{CH}_3\text{CN–CH}_2\text{Cl}_2} \text{PdL}_2 + \text{Products} \qquad (3)$$

also treated in this solvent with increasing amounts of HL·I$_2$. Despite all our attempts, **3** remained unchanged.

Although complex **3** is known in the literature,[3g,10] its crystal structure has not been reported to date, and the complex has only partly been investigated. Moreover, an increased interest in complexes bearing this class of ligands has recently emerged, in view of their potential applications in catalysing the carbonylation of methanol to ethanoic acid.[11] Therefore we have enlarged our study on **3** to characterise the com-

Table 1 Selected interatomic distances (Å) and angles (°) for complex **3**[a]

Pd–S(1)	2.3478(8)	Pd–S(2)	2.3333(8)
P(1)–S(1)	2.0255(13)	P(2)–S(2)	2.0258(11)
P(2)–N	1.595(3)	P(1)–N	1.597(3)
P(1)–C(1A)	1.803(3)	P(1)–C(1B)	1.806(3)
P(2)–C(1C)	1.807(3)	P(2)–C(1D)	1.809(3)
S(1)···S(2)	3.5519(2)	S(1)···S(2)′	3.049(2)
S(2)–Pd–S(1)	98.71(3)	S(2)–Pd–S(1)′	81.29(3)
P(1)–S(1)–Pd	99.34(4)	P(2)–S(2)–Pd	109.33(4)
N–P(1)–S(1)	115.59(11)	N–P(2)–S(2)	117.27(11)
P(2)–N–P(1)	122.2(2)		
N–P(1)–C(1B)	109.9(2)	N–P(1)–C(1A)	106.9(2)
C(1A)–P(1)–S(1)	105.90(12)	C(1B)–P(1)–S(1)	108.75(12)
C(1A)–P(1)–C(1B)	109.6(2)		
N–P(2)–C(1D)	111.8(2)	N–P(2)–C(1C)	106.0(2)
C(1C)–P(2)–S(2)	105.15(11)	C(1D)–P(2)–S(2)	110.33(13)
C(1D)–P(2)–C(1D)	105.3(2)		

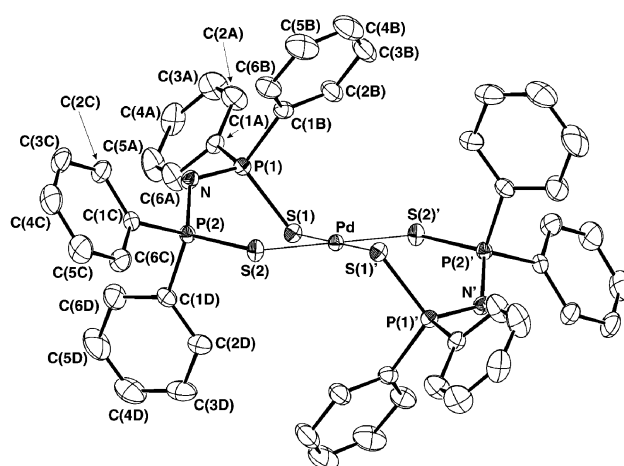[a] Primed and unprimed atoms are related by an inversion centre.

Fig. 2 Crystal structure of complex **3** as a ZORTEP[8d] drawing. Hydrogen atoms have been omitted for clarity. Thermal ellipsoids are drawn at 30% probability.

plex by X-ray single-crystal diffraction, FT-IR spectroscopy, electrochemical measurements, and then hybrid-DFT calculations on the simpler Pd[H$_2$P(S)NP(S)H$_2$]$_2$ **4** model complex.

Crystallographic studies

A ZORTEP[8d] view of compound **3** is given in Fig. 2. The central Pd^{II}, positioned upon a crystallographically imposed centre of symmetry, shows a distorted square-planar geometry. Its coordination sphere is occupied by four sulfur atoms belonging to two equivalent Ph$_2$P(S)NP(S)Ph$_2$ (L) anions acting as bidentate ligands, with Pd–S bond lengths of 2.3478(8)–2.3333(8) Å and S–Pd–S angles of 81.29(3)–98.71(3)° (see Table 1). Despite the deviations imposed by the ligand "bite" SPNPS on the coordination geometry of the metal, which lead to an *intra*-molecular non-bonding S(1)···S(2)′ interaction of 3.049 Å, the four sulfur atoms bind the palladium cation to define an almost perfect rectangular array with S(1)–S(2)–S(1)′ and S(2)–S(1)–S(2)′ angles of 90.36 and 89.64°, respectively. The sulfur atoms are also quite coplanar with both Pd and P(2) atoms (mean deviation 0.062 Å), while the PdSPNPS ring adopts a pseudo-boat conformation. P(2) and S(1) act respectively as the "bow" and "stern" of the boat, with deviations of 0.6283(12) and 1.1659(11) Å from the mean NS(2)P(1)Pd plane. The dihedral angle between the named plane and N(1)P(2)S(2) [PdS(1)P(1)] is 41.72(5)° [56.90(5)°]. While the overall structure of **3** is quite similar to that of the related complex Pd[Ph$_2$-

Table 2 Comparative structural data (bond lengths Å and angles °) for **HL**, **KL** and complexes **3**, **5**, **6** and **7**

Compound	Pd–S(Se)	P–S(Se)	P–N	S–Pd–S (Se–Pd–Se)	N–P–S(Se)	P–N–P	Ref.
Ph₂P(S)NHP(S)Ph₂ **HL**		1.937(1)	1.683(2)		115.49(9)	132.68(14)	13(*b*)
		1.950(1)	1.672(2)		114.59(9)		
K[Ph₂P(S)NP(S)Ph₂] **KL**		1.978(1)	1.592(2)		120.7(1)	128.6(2)	3(*b*)
Pd[Ph₂P(S)NP(S)Ph₂]₂ **3**	2.3478(8)	2.0255(13)	1.595(3)	98.71(3)	115.59(11)	122.2(2)	This work
	2.3333(8)	2.0258(11)	1.597(3)		117.27(11)		
Pd[Ph₂P(Se)NP(Se)Ph₂]₂ **5**	2.434(2)	2.178(3)	1.561(12)	99.3(1)	115.7(4)	122.9(5)	12
	2.457(2)	2.189(3)	1.621(11)		119.1(4)		
Pd[Prⁱ₂P(S)NP(S)Prⁱ₂]₂ **6**	2.341(3)	2.023(2)	1.588(4)	100.7(1)	117.1(1)	130.2(2)	2(*e*)
	2.347(1)	2.030(2)	1.597(4)		119.1(2)		
Pd[{Prⁱ₂P(S)NP(S)Prⁱ₂}-{Prⁱ₂P(S)NHP(S)Prⁱ₂}]Cl **7**							
Ring A *a*	2.353(4)	1.976(5)	1.64(1)	99.2(1)	111.6(4)	128.7(6)	2(*e*)
	2.359(3)	2.008(5)	1.65(1)		115.8(4)		
Ring B *a*	2.314(3)	2.040(5)	1.587(10)	100.5(1)	110.5(2)	128.2(7)	
	2.329(3)	2.045(4)	1.590(10)		110.6(1)		

a Ring A and B denote the protonated and deprotonated ligands respectively.

P(Se)NP(Se)Ph₂]₂ **5**[12], which is formally obtained by substitution of sulfur with selenium in the ligand **HL**, a comparison of the structures shows differences that are clearly associated with the larger atomic radius of selenium compared to sulfur. In fact, upon substitution of sulfur with selenium in the ligand anion, the mean Pd–X (X = S or Se) distances, the X–Pd–X angles, and the X(1)⋯X(2)′ distances increase by 0.105(3) Å, 0.59(10)° and 0.104(10) Å respectively (see Table 2). The metal-bonded atom size seems to have no influence on the conformation of the metallorganic ring PdXPNPX, which is probably controlled by the steric effects of the organic substituents on the phosphorus. This is strongly suggested both by the same conformation exhibited by the six-membered ring in related compounds **3**, **5**,[12] [Pd(Prⁱ₂P(S)NP(S)Prⁱ₂)₂] **6**[2e] and [Pd{(Prⁱ₂P-(S)NP(S)Prⁱ₂}{Prⁱ₂P(S)NHP(S)Prⁱ₂}]Cl **7**,[2e] as well as by the values of the dihedral angles PdX(1)P(2)X(2)–P(2)NP(1)X(1), which are equal within experimental error in **3**, **5** [60.31(4) and 58(1)°, respectively] and in **6**, **7** [47(1)°]. Compared to the neutral ligand **HL**,[13] the P–S bond lengths increase in compound **3**, being 2.025(1)–2.026(1) Å and 1.937(1)–1.950(1) Å in **3** and **HL** respectively, while the P–N distances are shortened [1.597(3)–1.595(3) *vs.* 1.672(2)–1.683(2) Å] and the P–N–P angle is contracted [122.2(2) *vs.* 132.68(14)°]. Although far from showing planar geometry, the PdSPNPS ring conformation seems to cause an increase in the π electron delocalisation over the fragment, as a result of the metal coordination. This is a recurrent motif in R₂P(S)NP(S)R₂–metal complexes and has been observed in tetrahedral,[2c,g,3a,c,g] square planar,[2e,3c,12] and square pyramidal[5a] M[R₂P(X)NP(X)R′₂]₂ complexes with di- and tri-valent metal ions [M = Co,[2c,g,3a] Ni,[3c,g,12] Pt,[2e,12] Pd,[2e,12] Zn,[3g] Cd,[3g] or Sb;[5a] X = S,[2c,e,3a,c,g,5a,12] or Se;[12] R(R′) = Me(Me),[12] Ph(Ph),[3a,c,5a,12] Ph(Me),[2c,3c] or Prⁱ(Prⁱ)[2f,3g]], thus suggesting remarkable insensitivity of the bond geometry of the MXP-NXP fragment with respect to the coordination geometry and the charge of the metal ion.

FT-IR studies

The two types of complex Pd(HL)I₂ and PdL₂ are readily distinguishable by IR spectroscopy,[10,14] since upon coordination **HL** and **L** feature a different π-electron delocalisation over the chelating ring SPNPSM, with the result that a significant change in the PN and PS bond order is expected. P–N stretching vibrations in the "free" ligand **HL** occur at 922 and 781 cm⁻¹, within the expected frequency range for single-bonded P–N stretching modes, whereas for its sodium salt Na**L** the higher wavenumber band appears at 1199 cm⁻¹, in the usual P=N stretching region, and the lower at 808 cm⁻¹.[10,14] P–S stretching vibrations in free **HL** have been identified at 689 and 650 cm⁻¹ (antisymmetric and symmetric stretching modes

respectively), whereas in Na**L** they are found at significantly lower wavenumbers: 598 and 570 cm⁻¹.[10,14] The frequency shifts are consistent with a decrease in P–S bond order as a consequence of the formation of the anionic **L** species. For **1** the positions of the PN and PS bands are consistent with those of **2**. The ν(PN) stretching frequencies fall at 915, 801 cm⁻¹ for **1** and 899, 818 cm⁻¹ for **2**,[10] whereas the ν(PS) are found at 597, 587 cm⁻¹ for **1** and 600, 592 cm⁻¹ for **2**.[10] For **1** the N–H vibration is not detectable, probably because it is greatly affected by intermolecular hydrogen-bonding interactions such as those in **7** where the chloride counter ion is hydrogen bonded to the protonated nitrogen (H⋯Cl 2.24, N⋯Cl 2.93 Å, N–H⋯Cl 139°).[2e] As expected from the structural data, the IR spectrum of **3** is indicative of a complex which features both an increased P–N and a reduced P–S bond order compared to those of the "free" ligand. Consequently ν_{asym}(PNP), which is the more sensitive to ligand complexation, falls at 1161 cm⁻¹, and ν(PS) at 571, 565 cm⁻¹. The magnitude of such shifts is in accordance with those of analogous Ph₂P(S)NP(S)Ph₂ complexes of formula ML₂ (M = Co, Cu, Fe or Mn) and with that found for **6**.[2e]

Electrochemistry

The redox properties of complex **3** have been monitored by cyclic voltammetry in CH₂Cl₂ solution (0.1 mol dm⁻³ Buⁿ₄-NBF₄) in the range +1.6 to −1.6 V, where the ligand **HL** is electrochemically inactive. One quasi reversible reduction was observed at $E_{1/2}$ = −0.99 V and one irreversible oxidation at E_{pa} = +1.24 V *vs.* Ag–AgCl. Coulometric measurements in CH₂Cl₂ indicate that both processes are monoelectronic and can presumably be assigned to the couples Pdᴵᴵ–Pdᴵ and Pdᴵᴵ–Pdᴵᴵᴵ respectively. All attempts to characterise the oxidation and reduction products have been unsuccessful. A cyclic voltammogram of I₂ in CH₂Cl₂ solution shows an irreversible reduction process at E_{pc} = −0.05 V (ΔE_p = 0.45 V) and a quasi reversible oxidation at E_{pa} = + 0.7 V (ΔE_p = 0.19 V, scan rate 100 mV s⁻¹) *vs.* Ag–AgCl (Fig. 3a). Coulometric measurements at controlled potential confirm that both are two-electron processes, and can therefore be tentatively assigned to the couples I₂–2I⁻ and I₂–2I⁺ respectively. On adding **HL** to the I₂ solution up to a 1 : 1 **HL** : I₂ molar ratio the cyclic voltammogram shown in Fig. 3(b) is recorded. This does not change on adding an excess of **HL** up to a 3 : 1 **HL** : I₂ molar ratio. The irreversible reduction at −0.19 V (ΔE_p = 0.32 V) and the irreversible oxidation at +0.95 V (ΔE_p = 0.30 V) have been verified to be two-electron processes by coulometric measurements and can be assigned to the couples **HL**·I₂–2I⁻ and **HL**·I₂–2I⁺ respectively. It seems, therefore, that from a redox point of view diiodine is reduced to I⁻ more easily than in the presence of **HL**. Further-
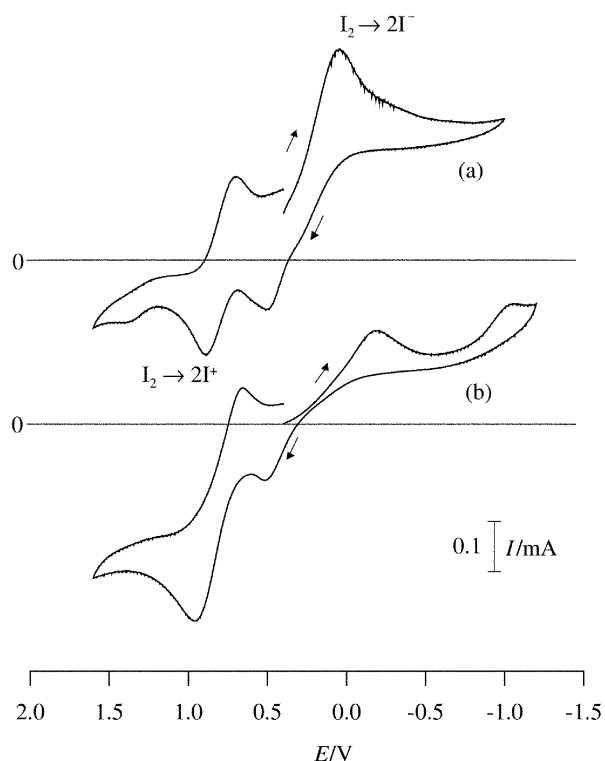
Fig. 3 Cyclic voltammograms of (a) I_2 in CH_2Cl_2, (b) after addition of an equimolecular amount of HL. Potential scanning in the cathodic direction starting from +0.4 V. Scan rate 100 mV s^{-1}; supporting electrolyte 0.1 mol dm^{-3} Bu$_4^n$NBF$_4$.

more, the reaction of palladium powder either with I_2 or HL in Et$_2$O leaves the palladium unchanged. All this leads to the conclusion that, in this case, the contemporary presence of HL and I_2 is necessary to promote oxidation of Pd^0 to Pd^{II} even though HL does not activate I_2 towards reduction to I$^-$.

Quantum-chemical calculations

In order better to understand the electronic nature of the complex **3**, hybrid-DFT calculations[9b] were performed on a model complex Pd[H$_2$P(S)NP(S)H$_2$]$_2$ **4**, in which the phenyl groups have been replaced by hydrogen atoms. Among the various types of theoretical calculations, DFT calculations[9b] are assuming a primary role since they yield encouraging results with inorganic compounds containing transition metals,[15a] either in their ground or excited state.[15b] The pVDZ basis sets of Schafer *et al.*[9f] for the ligand atoms and the Hay–Wadt basis set with ECP[9g,h] for the palladium atom have recently been used, since they gave excellent results on molecules with a high degree of electron delocalisation.[16] Geometry optimisation, which was performed starting from the structural data of **3**, correctly led to a molecule where the central metal ion is coordinated in a distorted square-planar fashion and the hexatomic metallacycle SPNPSPd assumes a boat conformation with a sulfur and a phosphorus atom, lifted with respect to the plane described by the remaining atoms of the metallacycle. A selection of optimised bond lengths and angles are reported in Table 3 along with data from the model [H$_2$P(S)NP(S)H$_2$]$^-$ **I**. A comparison between the bond distances calculated for **4** and the corresponding values calculated for the anion **I**, previously reported by us using the same hybrid functional and basis sets,[3a] show an easily foreseeable lengthening of the P–S bond lengths (by 0.07 Å). Upon complexation, the P–N bond lengths are correspondingly lengthened (by 0.01 Å respectively), and the P–N–P angle narrows. A comparison between the bond lengths and angles for **4** and those determined in the crystal structure of **3** shows that the values within the metallacycle are almost identical, with the only exception of the sulfur–metal bond distances,

Table 3 Selected calculated bond lengths (Å) and angles (°) for model compounds **4** and **I**[a]

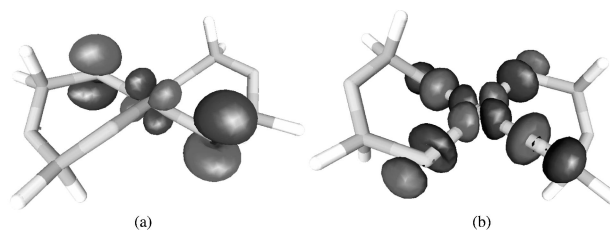|	**4**		**I**
Pd–S	2.425	2.434	
P–S	2.049	2.051	1.979
N–P	1.615	1.617	1.608
S–Pd–S	99.47		
S–Pd–S′	80.53		
P–S–Pd	105.41		100.66
N–P–S	120.28		117.50	126.96
P–N–P	120.75		144.14

[a] Values from Ref. 3(*a*).

Fig. 4 MOLDEN 3.6[9i] perspective drawings of the Khon–Sham HOMO (a) and LUMO (b) for the model compound **4**.
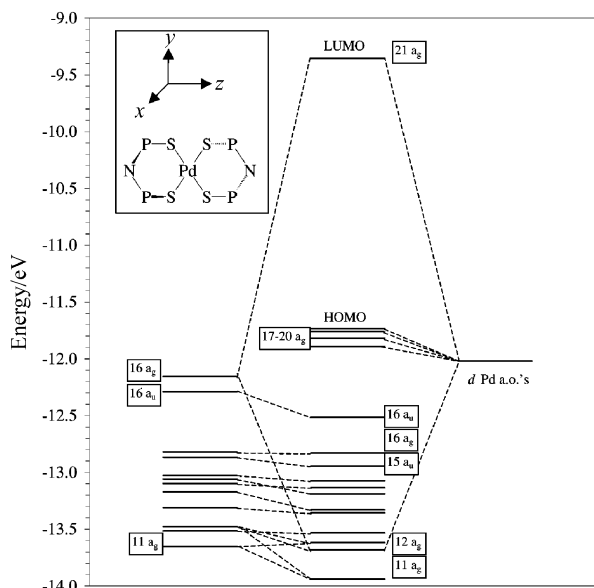

Fig. 5 EHT-Interaction diagram showing the interaction between the orbitals of the two ligand units **I** (left) and the palladium(II) atomic orbitals; FMO labelling refers to the C_i point group. The dashed lines connect FMOs which contribute at least 25% to the formation of molecular orbitals.

which are slightly overestimated, as previously found in similar compounds.[13] The HOMO (Fig. 4) consists of a molecular π orbital formed by an antisymmetric combination of two p$_z$ sulfur orbitals belonging to the two ligand units with the metal d$_{yz}$ atomic orbital. On the contrary, the LUMO is an antibonding σ orbital, in which the main contribution comes from the sulfur in-plane p orbitals and the palladium d$_{xy}$ atomic orbital. Based on the calculations performed on the model anion **I**,[3a] this orbital can qualitatively be considered as an antisymmetric combination of the HOMOs of the two ligands with the appropriate d atomic orbital.

In order better to understand the interaction between the metal ion and the ligands, a qualitative interpretation can be obtained from the fragment molecular orbital approach (FMO) within the extended Hückel theory (EHT) formalism. Using the

FMO approach, an interaction diagram can be constructed (Fig. 5) showing the interaction between the metal ion atomic orbitals and the fragment orbitals of the two ligands. The EHT energy levels for the fragments and for the complex were obtained using the DFT-optimised geometry, regularised to preserve the inversion centre. The five degenerate d-orbital energy levels of Pd^{II} are shown on the right hand side of Fig. 5, while the FMOs of the two ligand units are represented on the left. As the five degenerate d orbitals of the d^8 metal ion interact with the FMOs of the ligands they mix and split into five MOs, with the four occupied orbitals [in which the main contribution comes from the $d_{x^2-y^2}$(61), d_{xy}(46), d_{xz}(43) and d_{z^2}(62%) atomic orbitals, respectively] in a very short range of energy. These orbitals are slightly destabilised by antibonding interaction with the FMOs of the **I** moieties; the d_{yz} orbitals become the lowest unoccupied MOs, depending on the results obtained at the Hybrid-DFT level.

Acknowledgements

References

1 (a) S. M. Godfrey, N. Ho, C. A. McAuliffe and R. G. Pritchard, *Angew. Chem.*, *Int. Ed. Engl.*, 1996, **33**, 2344; (b) F. Bigoli, P. Deplano, M. L Mercuri, M. A. Pellinghelli, G. Pintus, M. A. Serpe and E. F. Trogu, *Chem. Commun.*, 1998, 2351; (c) F. Bigoli, P. Deplano, F. A. Devillanova, V. Lippolis, M. L. Mercuri, M. A. Pellinghelli and E. F. Trogu, *Inorg. Chim. Acta*, 1998, **267**, 115; (d) C. A. McAuliffe, S. M. Godfrey A. G. Mackie and R. G. Pritchard, *Angew. Chem.*, *Int. Ed. Engl.*, 1992, **31**, 919; and references therein.

2 (a) D. J. Birdsall, J. Novosad, A. M. Z. Slawin and J. D. Woollins, *J. Chem. Soc.*, *Dalton Trans.*, 2000, 435; (b) D. J. Birdsall, A. M. Z. Slawin and J. D. Woollins, *Inorg. Chem.*, 1999, **38**, 4152; (c) C. Silvestru, R. Rösler, J. E. Drake, J. Yang, G. Espinosa-Pérez and I. Haiduc, *J. Chem. Soc.*, *Dalton Trans.*, 1998, 73; (d) I. Haiduc, *Coord. Chem. Rev.*, 1997, **158**, 325; (e) C. Silvestru and J. D. Woollins, *J. Chem. Soc.*, *Dalton Trans.*, 1996, 2893; (f) D. Cupertino, R. Keyte, A. M. Z. Slawin, D. J. Williams and J. D. Woollins, *Polyhedron*, 1996, **24**, 4441; (g) C. Silvestru, R. Rösler, I. Haiduc, R. Cea-Olivares and G. Espinosa-Pérez, *Inorg. Chem.*, 1995, **34**, 3352; (h) M. C. Gimeno, A. Laguna, M. Laguna, F. Sanmartin and P G. Jones, *Organometallics*, 1993, **12**, 3894, and references therein.

3 (a) M. C. Aragoni, M. Arca, A. Garau, F. Isaia, V. Lippolis, G. L. Abbati and C. Fabretti, *Z. Anorg. Allg. Chem.*, 2000, **626**, 1454; (b) A. M. Z. Slawin, J. Ward, D. J. Williams and J. D. Woollins, *J. Chem. Soc.*, *Chem. Commun.*, 1994, 421; (c) R. Rösler, C. Silvestru, G. Espinosa-Pérez, I. Haiduc and R. Cea-Olivares, *Inorg. Chim. Acta*, 1996, **241**, 47; (d) O. Siiman and H. B. Gray, *Inorg. Chem.*, 1974, **13**, 1185; (e) D. J. Williams, C. O. Quicksall and K. M. Barkigia, *Inorg. Chem.*, 1982, **21**, 2097; (f) O. Siiman,

M. Wrighton and H. B. Gray, *J. Coord. Chem.*, 1972, **2**, 159; (g) D. Cupertino, R. Keyte, A. M. Z. Slawin, D. J. Williams and J. D. Woollins, *Inorg. Chem.*, 1996, **35**, 2695; (h) A. Davison and E. S. Switkes, *Inorg. Chem.*, 1971, **10**, 837; and references therein.

4 C. G. Pernin and J. A. Ibers, *Inorg. Chem.*, 2000, **39**, 1216; C. G. Pernin and J. A. Ibers, *Inorg. Chem.*, 2000, **39**, 1222.

5 (a) M. Arca, A. Garau, F. A. Devillanova, F. Isaia, V. Lippolis, G. Verani, G. L. Abbati and A. Cornia, *Z. Anorg. Allg. Chem.*, 1999, **625**, 517; (b) O. Siiman, C. P. Huber and M. L. Post, *Inorg. Chim. Acta*, 1977, **25**, L 11; (c) O. Siiman and J. Vetuskey, *Inorg. Chem.*, 1980, **19**, 1672.

6 A Schmidpeter, R. H. Bohm and H. Groenger, *Angew. Chem.*, 1964, **76**, 870.

7 *International Tables for X-Ray Crystallography*, ed. T. Hanh, D. Riedel, Dordrecht, 1983.

8 (a) A. C. T. North, D. C. Phillips and F. S. Mathews, *Acta Crystallogr.*, *Sect. A*, 1968, **24**, 351; (b) A. Altomare, M. C. Burla, G. Camalli, G. Cascarano, C. Giacovazzo, A. Guagliardi and G. Polidori, *J. Appl. Crystallogr.*, 1994, **27**, 435; (c) G. M. Sheldrick, SHELXL 93, Program for Crystal Structure Refinement, University of Göttingen, 1993; (d) L. Szolnai, Ortep Program for DOS, University of Heidelberg, 1997.

9 (a) M. J. Frisch, G. W. Trucks, H. B. Schlegel, P. M. W. Gill, B. G. Johnson, M. A. Robb, J. R. Cheeseman, T. A. Keith, G. A. Petersson, J. A. Montgomery, K. Raghavachari, M. A. Al-Laham, V. G. Zakrzewski, J. V. Ortiz, J. B. Foresman, C. Y. Peng, P. Y. Ayala, M. W. Wong, J. L. Andres, E. S. Replogle, R. Gomperts, R. L. Martin, D. J. Fox, J. S. Binkley, D. J. Defrees, J. Baker, J. P. Stewart, M. Head-Gordon, C. Gonzalez and J. A. Pople, GAUSSIAN 94 (Revision D.1 & E.1), Gaussian, Inc., Pittsburgh PA, 1995; (b) J. Labanowsky and J. Andzelm, in *Density Functional methods in Chemistry*, Springer-Verlag, New York 1991; (c) A. D. Becke, *J. Chem. Phys.*, 1993, **98**, 1372; (d) A. D. Becke, *J. Chem. Phys.*, 1993, **98**, 5648; (e) C. Lee, W. Yang and R. G. Parr, *Phys. Rev. B*, 1988, **37**, 785; (f) A. Schafer, H. Horn and R. Alhrichs, *J. Chem. Phys.*, 1992, **97**, 2571; (g) P. J. Hay and W. R. Wadt, *J. Chem. Phys.*, 1995, **82**, 270; (h) T. H. Dunning, Jr. and P. J. Hay, in *Methods of Electronic Structure, Theory, Vol. 2*, ed. H. F. Schaefer III, Plenum Press, Oxford, 1977; (i) G. Schaftenaar and J. H. Noordik, MOLDEN 3.6: a pre- and post-processing program for molecular and electronic structures, *J. Comp.-Aided Mol. Design*, 2000, **14**, 123; (j) R. Hoffmann and W. N. Libscomb, *J. Chem. Phys.*, 1962, **36**, 2179; (k) C. Mealli and D.M. Proserpio, *J. Chem. Educ.*, 1990, **67**, 399; (l) H. Fujimoto and R. Hoffmann, *J. Chem. Phys.*, 1974, **78**, 1167.

10 G. P. McQuillan and I. A. Oxton, *Inorg. Chim. Acta*, 1978, **29**, 69.

11 M. J. Baker, M. F Gilles, A. G. Orpen, M. J. Taylor and R. J. Watt, *J. Chem. Soc.*, *Chem. Commun.*, 1995, 197; J. R. Dilworth, J. R. Miller, N. Wheatley, M. J. Baker and J. G. Sunley, *J. Chem. Soc.*, *Chem. Commun.*, 1995, 1579.

12 P. Bhattacharyya, J. Novosad, J. Phillips, A. M. Z. Slawin, D. J. Williams and J. D. Woollins, *J. Chem. Soc.*, *Dalton Trans.*, 1995, 1607.

13 (a) H. Nöth, *Z. Naturforsch.*, *Teil B*, 1982, **37**,1491; (b) S. Husebye and K. Maartmann-Moe, *Acta Chem. Scand.*, *Ser. A*, 1983, **37**, 439; (c) P. B. Hitchcock, J. F. Nixon, I. Silaghi-Dimitrescu and I. Haiduc, *Inorg. Chim. Acta*, 1985, **96**, 77.

14 R. Czernuszewicz, E. Maslowsky, Jr. and K. Nakamoto, *Inorg. Chim. Acta*, 1980, **40**, 199.

15 (a) C. Adamo and F. Lelj, *J. Chem. Phys.*, 1995, **103**, 10605; (b) C. Dual, *J. Quantum Chem.*, 1994, **52**, 867.

16 M. Arca, F. Demartin, F. Devillanova, A. Garau, F. Isaia, F. Lelj, V. Lippolis, S. Pedraglio and G. Verani, *J. Chem. Soc.*, *Dalton Trans.*, 1998, 3731; M. C. Aragoni, M. Arca, F. Demartin, F. Devillanova, A. Garau, F. Isaia, F. Lelj, V. Lippolis and G. Verani, *J. Am. Chem. Soc.*, 1999, **121**, 7098.